LAWRENCE
LIVERMORE
NATIONAL
LABORATORY

LLNL-PROC-654799

The Guider and Wavefront Curvature Sensor Subsystem for the Large Synoptic Survey Telescope

V. Riot, K. Arndt, C. Claver, P. Doherty, K. Gilmore, P. Hascall, S. Herrmann, I. Kotov, P. O'Connor, J. Sebag, C. Stubbs, M. Warner

May 22, 2014

SPIE: Astronomical Telescopes and Instrumentation 2014
Montreal, Canada
June 22, 2014 through June 27, 2014

Disclaimer

This document was prepared as an account of work sponsored by an agency of the United States government. Neither the United States government nor Lawrence Livermore National Security, LLC, nor any of their employees makes any warranty, expressed or implied, or assumes any legal liability or responsibility for the accuracy, completeness, or usefulness of any information, apparatus, product, or process disclosed, or represents that its use would not infringe privately owned rights. Reference herein to any specific commercial product, process, or service by trade name, trademark, manufacturer, or otherwise does not necessarily constitute or imply its endorsement, recommendation, or favoring by the United States government or Lawrence Livermore National Security, LLC. The views and opinions of authors expressed herein do not necessarily state or reflect those of the United States government or Lawrence Livermore National Security, LLC, and shall not be used for advertising or product endorsement purposes.

The Guider and Wavefront Curvature Sensor Subsystem for the Large Synoptic Survey Telescope

Vincent J. Riot*[a], Kirk Arndt[b] , Chuck Claver[c], Peter E. Doherty[d], D. Kirk Gilmore[e], Patrick A. Hascall[e], Sven Herrmann[e], Ivan Kotov[f], Paul O'Connor[f], Jacques Sebag[c], Christopher W. Stubbs[d] , Michael Warner[g]

[a]Lawrence Livermore National Laboratory, 7000 East Ave., Livermore, CA, USA; [b]Physics Department, Purdue Univ., 525 Northwestern Ave, West Lafayette IN USA; [c]LSST Corporation, 933 N. Cherry Ave, Tucson AZ USA; [d]Department of Physics, Harvard University, Cambridge, MA, USA; [e]SLAC National Accelerator Laboratory, 2575 Sand Hill Rd., Menlo Park, CA USA; [f]Brookhaven National Laboratory, Upton, NY, USA; [g]Cerro Tololo Interamerican Observatory, La Serena, Chile

ABSTRACT

The Large Synoptic Survey Telescope instrument include four guiding and wavefront sensing subsystems called corner raft subsystems, in addition to the main science array of 189 4K x 4K CCDs. These four subsystems are placed at the four corners of the instrumented field of view. Each wavefront/guiding subsystem comprises a pair of 4K x 4K guide sensors, capable of producing 9 frames/second, and a pair of offset 2K x 4K wavefront curvature sensors from which the images are read out at the cadence of the main camera system, providing 15 sec integrations. These four guider/wavefront corner rafts are mechanically and electrically isolated from the science sensor rafts and can be installed or removed independently from any other focal plane subsystem. We present the implementation of this LSST subsystem detailing both hardware and software development and status.

Keywords: LSST, guide sensors, wavefront sensors, ground-based telescope

1. INTRODUCTION

The 8.4 m LSST will be constructed on the El Penon peak on Cerro Pachon in northern Chile. Its three large telescope mirrors will be actively controlled to minimize distortions. The telescope mount will be a compact, stiff structure especially designed to reduce image motion. The LSST Camera, with three refractive lenses and a 9.6 square degree field of view, will be the largest digital camera ever constructed. The LSST will take pairs of 15 second exposures of each field, separated by a 2 second readout. Operational simulations demonstrate that the LSST can deliver a uniform and deep 18,000 square degree survey with over 5.2 million exposures in ten years.

The Camera provides a 3.2 gigapixel flat focal plane array, tiled by 4K x 4K CCD sensors with 10 µm square pixels. The sensors are deep depleted, back illuminated devices with a highly segmented architecture that enables the entire array to be read out within the required 2 seconds. Detectors are grouped into rafts in 3 x 3 arrays, each containing its own dedicated electronics boards supporting 1x3 sensors per boards. The rafts are mounted on a silicon carbide grid inside a vacuum Cryostat, with an intricate thermal control system that maintains the CCDs at an operating temperature of -100ºC. The grid also contains four sets of guide sensors and wavefront sensors in "Corner Rafts" at the edge of the camera field. The entrance window to the Cryostat is the refractive lens L3, the third of three such lenses in the Camera. The other two lenses, L1 and L2, are mounted in an optics structure at the front of the Camera Body, which also contains a mechanical shutter and a Carousel assembly that holds five large optical filters.

The conceptual design[1] of the corner raft in the LSST camera relied on 2 CMOS sensors for guiding operations and a split sensor design based on two 2k x 4k CCD sensors assembled in a monolithic package. As part of the design and development effort, various trade-studies were completed to re-assess this conceptual design. The guide sensors conceptual design was evaluated against a CCD solution based on the same 4kx4k sensor used for the science array, the wavefront sensors conceptual design was evaluated against various arrangement providing intra and extra focal images, and the electronics was updated to address the overall thermal design of the LSST camera in a manner compatible with the science raft tower design.

*riot1@llnl.gov; phone 1 925 422-9798; LLNL-PROC-654799

2. CORNER RAFT FUNCTIONALITY

2.1 Role of the corner raft in the LSST

The corner raft sub-system is contained inside the LSST Camera as it needs access to the focal plane, but has a role in activities encompassing the entire operation of the telescope.

The corner raft sub-system is responsible for acquiring pixel data for the active optics system based on curvature wavefront sensing[2,3]. To support this activity, the corner raft sub-system must acquire intra and extra focal images at 4 locations at the edges of the focal plane that will be used by the Telescope Control System to estimate the wavefront and, through reconstruction, provide inputs to the active optics controller. Images are collected in parallel with the science images and follow the corresponding exposure time and cadence (nominally 15 second exposure and 2 second readout time).

The corner raft sub-system is also responsible for acquiring 8 small images centered on selected bright stars at a nominal 9Hz rate. These images are used to estimate the pointing variation during the exposure and provide input to the telescope control tracking system.

2.2 Corner raft specifications

The corner raft specifications for the LSST are captured within a set of two interface documents between the LSST telescope and the LSST camera. The guider system interface specifies the performances of the guide sensors as described in Table 1 and reflects the preliminary design approach.

Table 1. Guide sensor specifications.

Key requirement	Value
Pixel Size	10 µm square pixels
Readout Noise	9 e- rms
Integration time	50 ms
Frame Rate	9 Hz
Window size	50 x 50 pixels
Sensor Flatness/z-axis tolerance	+/-30 µm
Number of Guide Sensors	8

The guide sensor specifications have been set to ensure that the servo loop jitter for point spread functions on the sky better than 0.6 arc-sec FWHM will be less than 0.02 arc-sec FWHM. Based on the servo-loop implementation[4], this requirement can also be expressed as a single guide sensor rms centroid accuracy of 0.04arc-sec = 0.2 pixels with worst case flux of 800e- (u-band)

The wavefront system interface specifies the performances of the wavefront sensors as described in Table 2.

Table 2. Wavefront sensor specifications.

Key requirement	Value
Pixel Size	10 µm square pixels
Readout Noise	10 e- rms
Intra/Extra focal sensor separation	4 mm +/-0.1 mm
Integration time	15 s
Readout Time	2 s
Sensor Flatness	+/-15 µm

The current specification requires flexibility to adjust the intra to extra focal separation up to 4.8mm from the nominal 4mm separation. This will be set at the time of final assembly based on final analysis and tests.

The wavefront sensor mechanical alignment is tied to the science sensor array best fit plane as it is a critical component of wavefront correction. The details of the overall mechanical alignment requirements applicable to the corner raft are shown in Figure 1.

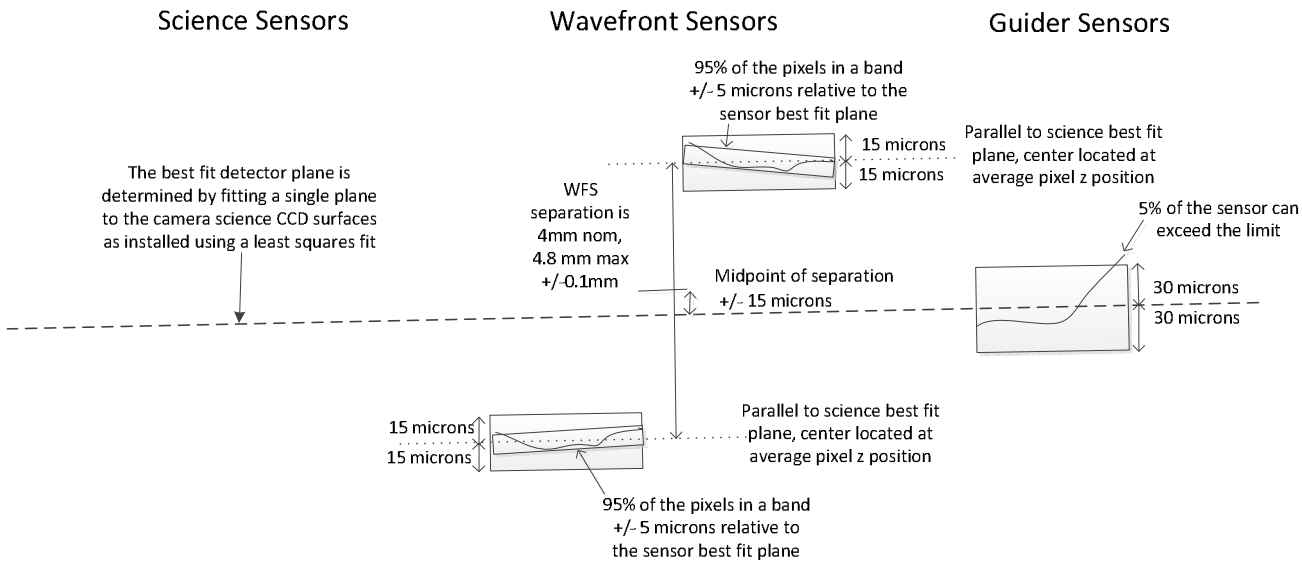

Figure 1. Corner raft sensor mechanical alignment and tolerance requirements.

3. CORNER RAFT GUIDE SENSORS

3.1 Guide sensors trade-study against the conceptual design

In order to reduce cost and complexity, a trade study was conducted to assess feasibility of using a science sensor CCD for guide operation as a replacement for an expensive CMOS sensor. Besides the cost reduction, various advantages were foreseen, mainly focusing on consistency of the readout electronics and scientific expertise tied to a single technology.

The pin-CMOS solution selected during the conceptual design (H4RG[5]) is attractive because it provides a straightforward means of reading out region-of-interest (ROI) windows due to its amplifier-per-pixel architecture and flexible addressing modes. Pixels can be reset at any time providing the electronic shuttering. In addition, the device is supported by a sophisticated control and data acquisition ASIC (SideCar[6]) offering compactness, low power, and full digital output. The SideCar can operate at low temperatures and would be located in the corner raft tower near the sensor. However, the H4RG sensor has several disadvantages compared to the proposed science sensor CCD: Read noise is 2X -- 3X larger; Unable to bin pixels to tradeoff read noise and spatial resolution; Cost about 3X greater. In addition, the use of pin-CMOS technology requires the development and support of a new precision package, a new front-end electronics chain, the associated mechanical and thermal interfaces, and a separate complement of spares.

The LSST team assessed the ability to repeatedly and rapidly read an arbitrarily-located region of interest (ROI) window and reviewed the impact of photon statistics, amplifier read noise and image smear in shutterless operation on centroid noise. The structure of the LSST science CCD is illustrated in Figure 2. It is a full-frame 4K × 4K device with 10μm pixels (0.2”/pixel) organized as 16 independent 2K × 0.5K segments, each with individual readout. The parallel (vertical) and serial (horizontal) clocks are common to all segments. The parallel clock readout rate is limited by RC time constants on the polysilicon parallel clock lines; the manufacturer estimates that the minimum parallel transfer time to be 16 μsec. The time to read out a ROI window depends on the location of the window relative to the amplifiers. For 50x50 pixel guide windows, the time to read out a window will be between 7ms and 54ms depending on the window position, which is compatible with a 50ms integration time at a 9Hz frame rate. Note that this readout time is dominated by the time to execute the parallel row shifts needed to transfer the window charge to the serial register. The maximum readout time can be reduced by requiring guide stars to be located within a restricted number of rows from the serial

register, at the expense of reduced area. In addition to the read noise, an additional source of centroid error in CCDs is image smear while the window is shifted to the readout amplifier and read out with open shutter. The guide window "box" will accumulate additional photoelectrons due to photons (from sky, sources, or stray/scattered light) or cosmic rays that are incident on pixels along the path taken by the guide window charge during its transport to the readout register. Those pixels are a small fraction (never more than 0.2%) of the sensor area and so the probability of them intercepting another bright source is low; in general the location of bright sources will be known in advance and the guide star can be chosen to avoid these interfering sources. Flux from sources dimmer than the guide star could contaminate the centroid. However, smeared charge from such sources is only integrated during the time the ROI window is shifted across their PSF. For any given pixel in the ROI the time spent shifting across an interfering source to the integration time is the parallel shift time divided by the integration time or 16μs/50ms = 3.2×10-4. Hence, the amount of smeared, structured charge that could interfere with the centroid estimate will be negligible

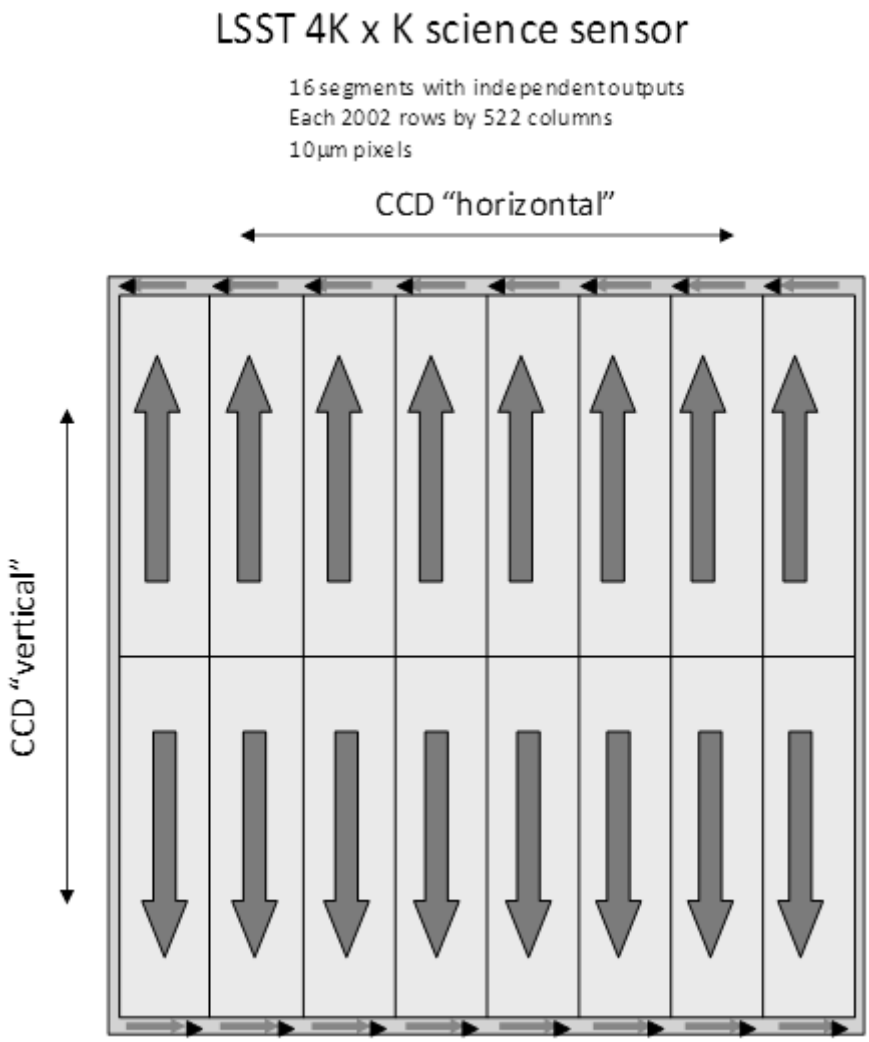

Figure 2. The LSST CCD sensor structure.

The trade-study concluded that the 4K x 4K LSST science CCD with its 16-fold segmented readout structure can be operated as a guide sensor without degradation of centroid error performance. The loss of integration time resulting from the need to shift the guide window to the readout register is compensated by the CCD's superior read noise and ability to bin pixels compared to the H2RG CMOS hybrid sensor. Additionally, The CCD has higher QE, when compared to the CMOS, at both ends of the spectrum, which increases the worst case flux by 1.73 times. From this study, the LSST team adopted the use of science sensor CCDs as guide sensors.

3.2 CCD Guide sensor performance verification

In order to demonstrate the capability to meet the guide sensor requirement using the preliminary design, the LSST corner raft team has conducted some centroid noise measurement on an actual LSST prototype CCD from E2V. A spot projector was tightly focused on the center of segment 6 of a CCD250 device at two intensity levels covering 320ADU and 7100ADU (gain of 4.2e-/ADU) on the readout controller. The acquisition was performed using a Reflex controller with a frame rate of 9.2Hz and a guide window of 64x64 pixels. The Parallel line transfer was accomplished in ~11µs with 5ohm driver series resistance. Statistics were collected across 1000 frames with the specified 50ms integration time.

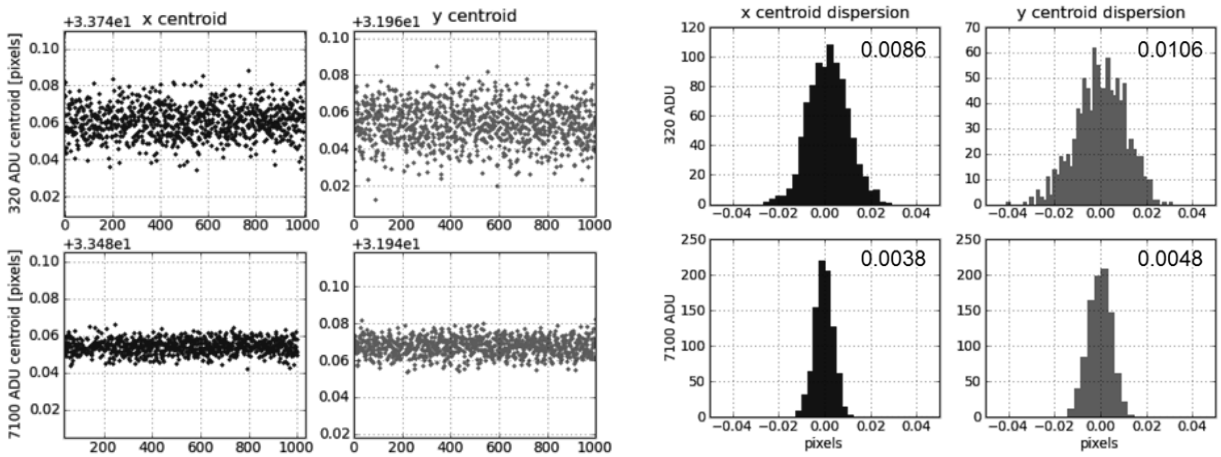

Figure 3. 1000 frames taken at 50ms Tint, 9.2Hz rate, and 2 intensities. The centroid position versus frame number is plotted on the left against frame numbers and the overall centroid dispersion histogram is plotted on the right. The requirement of 0.2 pixel FWHM is easily met.

3.3 Guide sensor design

Two guide sensors are located in each of the 4 corner rafts (total of 8 guide sensors – see Figure 4). The baseline design for guiders uses 4K x 4K LSST science CCD sensors with 10 micron pixels. The CCD sensors are deep-depletion, back-illuminated devices with a highly segmented architecture. The readout electronics are mounted on a custom printed circuit board and housed inside a metal enclosure for EMI shielding and heat transfer to the cold plate. A pair of flat flex cables (identical to those used connectivity in the science CCD array) mates to circuitry on the back-side of the CCD sensor package, and terminates in an 85-pin Nano-connector for connection to the readout electronics board.

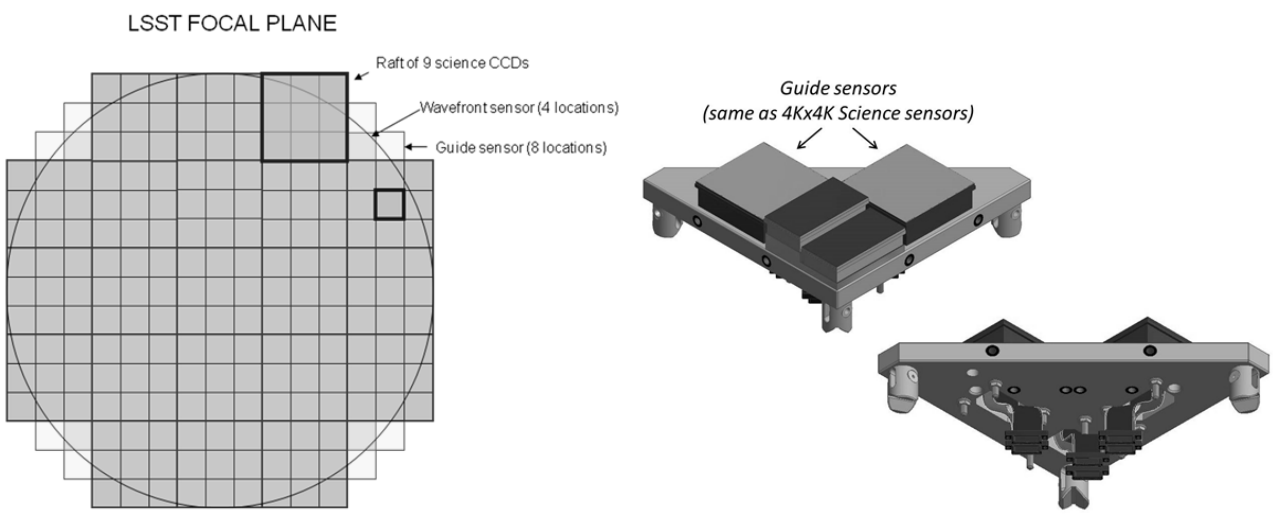

Figure 4. The LSST focal plane layout and Guide sensor assembly preliminary design

4. CORNER RAFT WAVEFRONT SENSORS

4.1 Wavefront sensors trade-study against the conceptual design

In order to reduce cost and complexity inferred by the conceptual design an extensive trade study was conducted to find any attractive alternative to the wavefront sensor implementation while maintaining the generation of appropriate intra and extra focal images. The following alternatives, ordered in increasing benefits, were compiled:

- Pistoning wavefront sensor for intra/extra focal images: it was assessed that wavefront reconstruction performance could be increased as the same star could be used for the intra and extra focal image. However this approach added extra complexity and risk due to the need for moving components.
- Tilted wavefront sensor for intra/extra focal images: A tilted 4k x 4k sensor was assessed as simplifying the sensor design. However, the tilt resulted in complex algorithm for re-construction as well as a reduction in performance beyond acceptable levels.
- Add optical elements over half of a 4k x 4k sensor to produce intra/extra focal images: various methods to generate the change in optical path for one half of the sensor were compiled, including a bi-refringent crystal, flat glass or dispersive hologram. However, the fast converging beam for the LSST (1.2 f#) produces significant aberration for those systems.
- One science sensor used for intra/extra focal image, wavefront sensor location used for the other one: this approach consisted of trading one science raft sensor adjacent to the corner raft to provide one of the intra/extra focal images. This sensor, being out of focus, cannot provide images useful for science and results in a 2.2% reduction in actual coverage. This was deemed too significant to be acceptable.
- Use the guide sensors for the two intra/extra wavefront sensors and the wavefront sensor for a single guide sensor (swap guide and wavefront sensor reserved area on the corner raft sub-system): This method implies that only one guide sensor is used in each corner and increases the guider centroid noise by the square root of two. In addition, the location of the two proposed wavefront sensors located at the edge of the field experiences vignetting beyond acceptable levels for more than 70% of the area. Additionally, the two sensors are not next to each other causing unacceptable issues with the wavefront reconstruction algorithm.
- Two 2Kx4K Sensors on different package: this approach was based on attempting to simplify the complex monolithic package of two 2k x 4k CCD sensors. The assembly of the package is to be done at the raft baseplate level simplifying the overall design. The need for required additional mounting hardware necessary to support two separate sensors has been analyzed and can be supported by a step plate. Additionally the need to have a late, one time separation distance adjustment can be also supported.

4.2 Wavefront sensor design

The LSST requires four wavefront sensors located in the corner rafts at the periphery of the focal plane (see Figure 4). A depiction of the wavefront sensor concept is shown in **Error! Reference source not found.**Figure 5. Two 2K x 4K segmented CCDs packages will be mounted on a “step plate” and offset relative to the science focal plane to produce intra and extra focal images. An offset of roughly +/- 2mm from the science focal plane is anticipated. Wavefront sensor CCDs will share the layout and processing of the science sensors, and have similar performance as science CCDs regarding quantum efficiency, point spread function, read noise, and readout speed. Detailed mechanical specifications such as fill factor, flatness, parallelism of the intra and extra focal sections, and temperature sensing will be validated by laboratory measurements.

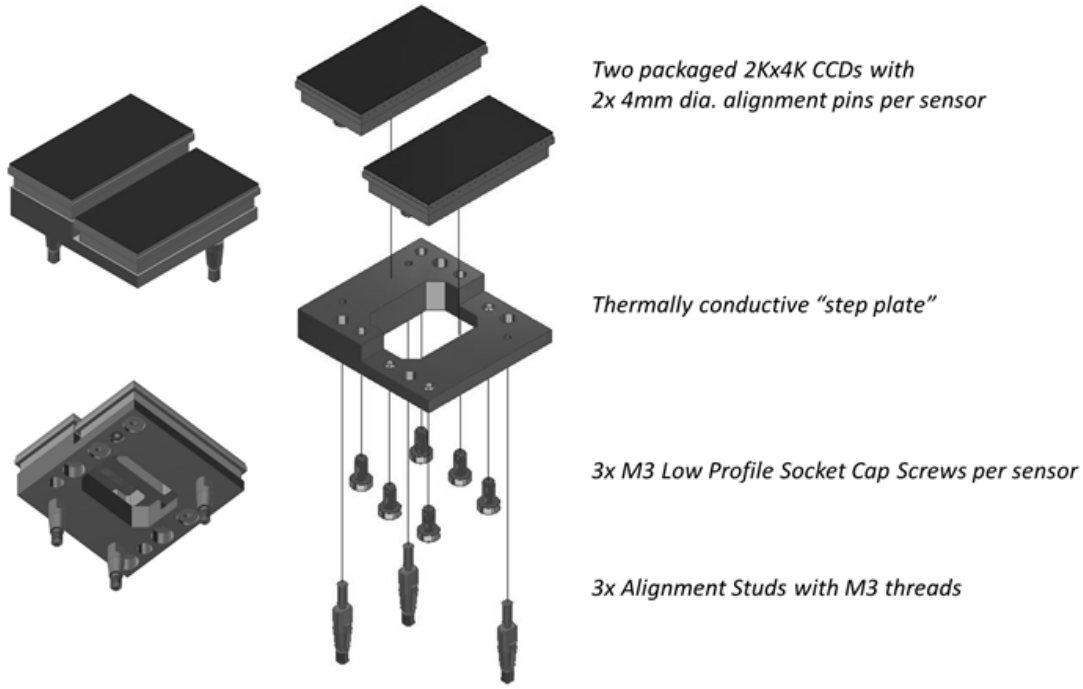

Figure 5. Wavefront sensor assembly preliminary design

5. CORNER RAFT MECHANICAL AND ELECTRICAL ASSEMBLY

5.1 Raft Design

Each sensor package will be mounted to the corner raft structure by means of 3 threaded stud/pin legs, Belleville washers and locking nuts. Removable, thermally-conductive spacer/shims that can be adjusted will be used to set the height of the sensor surfaces above the corner raft. Identical corner rafts will be mounted in four corner locations on the grid structure (which also supports the science rafts) by means of an adjustable 3-point ball-and-vee kinematic mount design. The design for this mount system is shown in Figure 6.

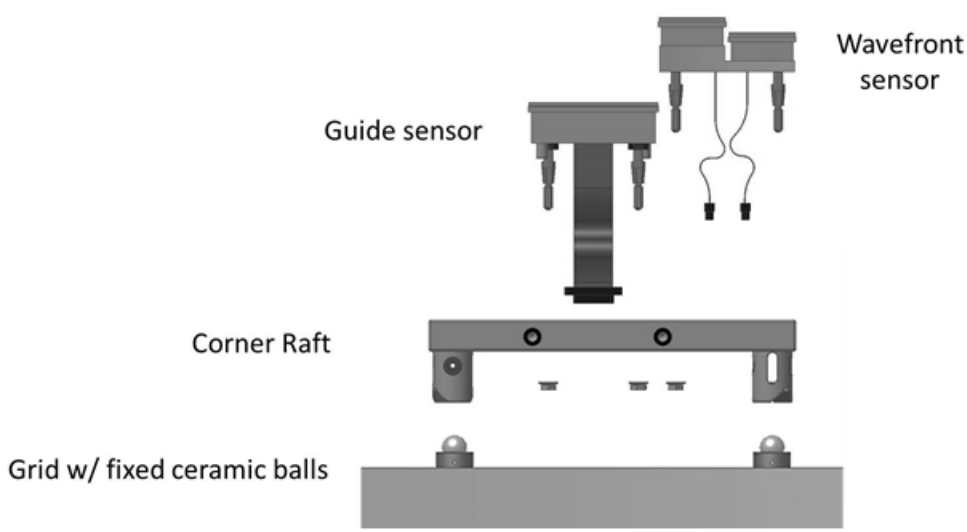

Figure 6. Side view of sensor-to-corner raft-to-grid mounting scheme

The back side of the corner raft features three radially-arrayed vees ground into the raft material. The vees uniquely define the position of the corner raft with respect to silicon-nitride ceramic balls that are fixed in cups mounted on the grid. This forms a kinematic connection that isolates the corner (and science) rafts from grid distortion due to external dynamic and transient loads, assembly tolerances, and to the expected thermal motions due to differential contraction during cooling. The corner rafts are held in position by springs that pre-load the corner rafts against their kinematic coupling to the grid, producing a uniform, invariant loading. The deflection of grid and corner raft due to the spring loading is compensated for during initial integration, and remains unchanged in operation, independent of camera orientation and temperature.

The grid, science rafts, and corner rafts will be manufactured from a silicon-carbide ceramic matrix composite. This material is used for lightweight and stable space-borne structures, including focal planes, optical benches, and mirrors. The high modulus, high thermal conductivity, near-zero expansion coefficient and improved fracture toughness of the ECM CeSiC® material makes it ideal for the grid, science raft, and corner raft structures. A closed-loop thermal control system will be used to adjust the temperature of the corner rafts instrumented with temperature sensors and make-up heaters, thereby maintaining a suitable and stable operating temperature for the sensors.

5.2 Tower Design

The LSST Camera cryostat contains four sets of guide sensors and wavefront sensors in corner rafts at the edge of the camera field (see Figure 4). Each Corner Raft sub-system contains one wavefront sensor and two guide sensors and dedicated front end electronics. The mechanical and thermal design of the corner rafts is as similar as possible to the science rafts.

The grid supports as little mass as possible—only the sensor rafts and their supports—to reduce gravity induced deflections. The tower is supported by a neighboring cryogenically-cooled "Cryoplate" at about -130C temperature. Each corner raft is thermally connected, but structurally decoupled from the tower by use of braided copper thermal straps to remove the electrical and radiant heat load from each Corner Raft and conduct it back to the cryoplate.

Front-end electronics for operating the wavefront and guide sensors are packaged within the volume behind the corner raft (similar to the science raft configuration) in the tower. Electrical connections between sensors and front-end electronics boards are made by flat flex circuit cables. The electronics boards are thermally connected to the cold plate at about -40C by thermally conductive straps. Details of the preliminary design for corner raft/towers for the LSST camera are shown in **Error! Reference source not found.**Figure 7.

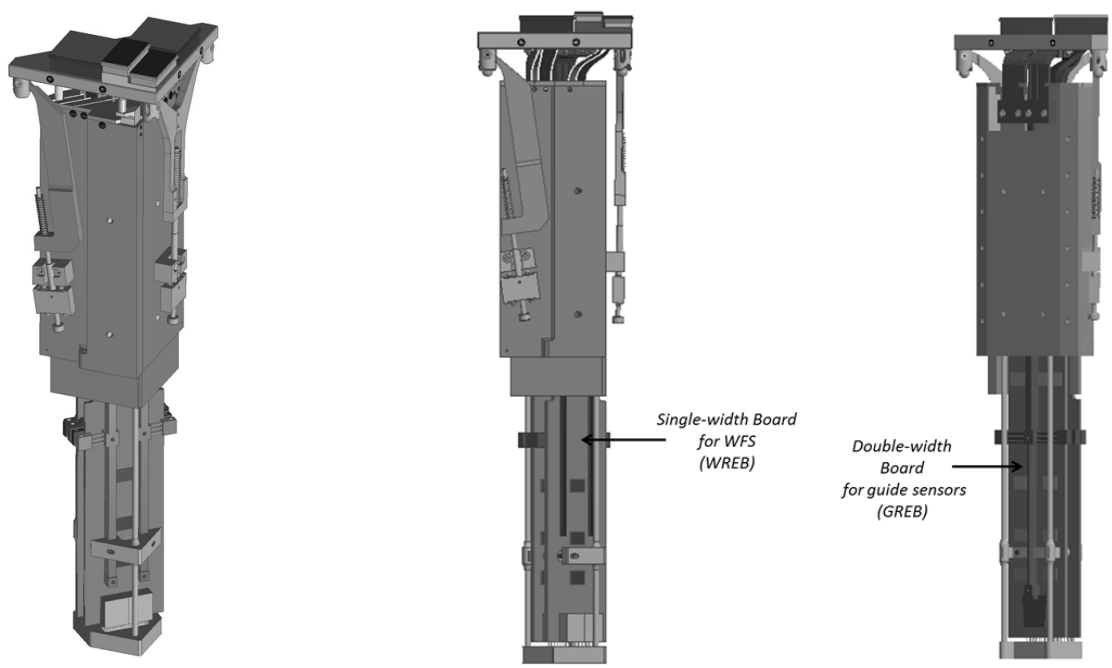

Figure 7. Corner raft tower design.

5.3 Electronics Design

The corner raft tower electronics provides all CCD biasing and clock signals, CCD signal amplification and low noise analog signal processing, digitization, data collection, and transmission of image and metadata to the DAQ. The corner raft tower electronics also has the responsibility for monitoring and reporting a variety of metadata such as supply voltages and currents, precision temperature measurements, and operating raft heaters to maintain the focal plane temperature. In addition, a significant ability to diagnose problems *in situ* will be part of the design. The video data from the CCDs will be transmitted via two high speed serial links (one for both guide sensors, one for the wavefront sensor) to the DAQ system. Analog to the dual functionality of the corner raft, namely guiding and wavefront sensing the electronic is partitioned into 2 PCBs: one for the operation of the two guide sensors at high frame rates with a total of 32 analog channels (GREB for Guide Raft Electrics Board) and one for the operation of the wavefront sensor with 16 channels (WREB for Wavefront Raft Electrics Board). The two different CCD types (for guide sensor and wavefront sensor) will be very similar in terms of segmentation and readout and therefore will be interchangeable with respect to the electronic. Therefore it is foreseen to utilize the same basic electronic block for both PCB types. Still, some optimization for the specific functionality will be implemented, especially to support the fast shift and region of interest readout for the guide sensors. The CCDs will be connected to the readout boards via polyimide flex leads. Length and layout of this connection is critical for noise and crosstalk performance.

Table 3.Corner raft tower readout electronics specifications.

Key requirement	GREB	WREB
Number of video channels	32	16
Readout noise contribution	< 3.65e- rms	< 3.65e- rms
Maximum signal level	180ke-	180ke-
Digitization	18bit	18bit
Channel to channel crosstalk	< 0.002	< 0.002
Readout size	50x50 pixel ROI	full frame
Integration time	> 50ms	15s
Readout time	< 61 ms	2s
Operational power	17.5W	9.5W

The high channel density video chain utilizes two types of application specific integrated circuits (ASIC): one for CCD biasing and clocking (CABAC[7]) and one for analog signal processing (ASPIC[8]). For the operation of a single CCD with 16 video channels two CABAC and two ASPIC chips are needed. The ASICs used are packaged in QFN-100 packages.

The CABAC (Clock and Bias ASIC for CCDs) is an ASIC realized in a specialized high voltage CMOS process, AMS 0.35um HV CMOS process (H35BAD3), which will provide the clock signals and most of the bias voltages for the CCD sensors. Each chip will provide high drive capability clock signals, three low current bias voltages, two high current programmable voltage sources for the CCD output drains, and an analog multiplexer to provide diagnostic and environmental feedback. The CABAC is programmed via a simple SPI serial protocol. The digital CCD clocks signals are provided via LVDS to the CABAC while the upper and lower clock rail voltages are delivered by regulators on the PCB,

The ASPIC (Analog Signal Processing ASIC) refers to the CCD Analogue Signal Processing Integrated Circuit implemented in the AMS 0.35um CMOS process. Its purpose is to amplify and filter the video signal coming from the CCD's in order to optimize the signal to noise ratio before digitization. The filtered analog signals are provided via differential output to the ADC drivers on the PCB. The ASPIC contains 8 video channels per chip and therefore two ASPIC chips are needed to read out one 16 channel CCD. The ASPIC implements video signal processing based on the dual slope integrator (DSI) scheme. Dual slope integrator processing combines correlated double sampling with CCD signal integration.

This allows adding both system benefits. Correlated double sampling, eliminating reset noise, removes *kT/C* and *1/f* noise while integration removes thermal noise. This scheme allows adding both system benefits and is performed by integrating first the CCD reference signal just after reset and then integrating the charge signal with opposite polarity (see Figure 8). The difference of these two integrations (with exactly the same integration time) provides the CCD signal with the *kT/C* and *1/f* noise contributions filtered.

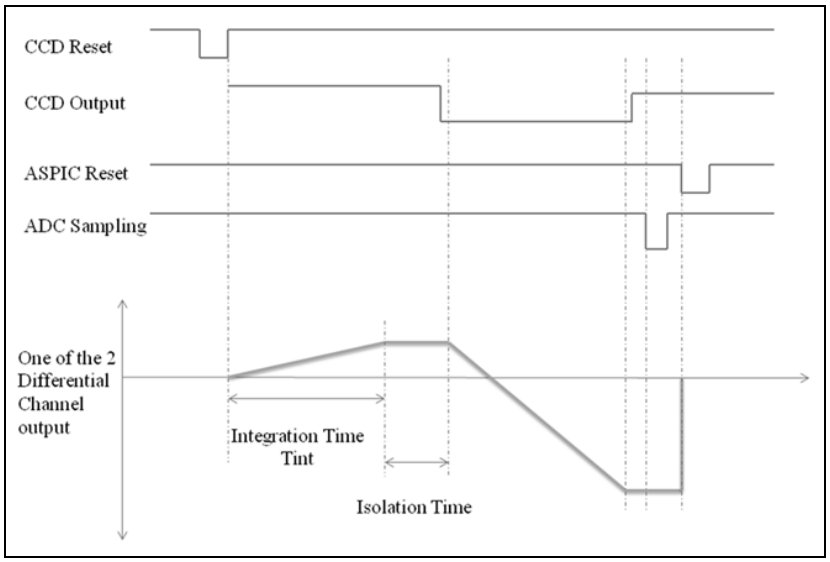

Figure 8. Dual slope integration scheme sequence.

The CCD will be AC coupled to the ASPIC through an external capacitance. A large clamp switch has been integrated to perform a DC level restore regularly. The biasing of the 16 CCD source follower outputs is implemented by discrete low noise JFET current sources

The output of the ASPIC is sent as a differential analog signal to a commercial differential buffer and 18-bit ADC for digitization. The ADC is rated for 1 MS/s but will be operated at the LSST pixel rate of about 500 kpixels/s. This pixel data from the single channel ADCs is fed as individual serial streams directly into the FPGA where the firmware combines the pixel data into packets to be sent out via the high speed serial link to the DAQ hardware in the Observatory Control Room. At the same time, sequencer logic in the FPGA firmware provides direct control of the timing of all the circuitry involved in the video chain: parallel and serial CCD clocks, clamps, resets, ramp up and down for the DSI scheme in the ASPIC and the A/D conversion timing – all based upon a common 100 MHz clock distributed from the DAQ hardware to each read out PCB of the LSST focal plane. The board also houses a number of regulators, DACs and power Op-amps to generate all fixed and programmable voltages required for all components on the PCB. In addition to the video chain there are numerous housekeeping and support tasks the WREB and GREB provide such as:

- hardware serial number
- monitor all temperature sensors, which are distributed on the REB, in the CCD sensor packages and integrated into the ASICs
- prepare meta-data packets for transmission to the DAQ.
- control and power the raft heaters
- dual 100 MS/s ADCs to look at any two signals available in any CABAC on the board – for instance to compare and tune timing of two serial clock edges
- protection circuitry for the CCD and hardware encoded power up sequencing

6. CONCLUSION

The mechanical and electrical design described here for the corner raft has been improved from the earlier conceptual design, is compatible with the physical constraints imposed by the LSST camera structure, and meets the performance requirements for both wavefront reconstruction and guiding. Using a consistent CCD sensor technology for both guider and wavefront sensors is providing significant cost reduction as well as a reduction in technical complexity by allowing the readout electronics to be based on the same custom integrated circuits. The LSST corner raft team has demonstrated through early testing that this approach will indeed satisfy all performance and functional requirements.

REFERENCES

[1] Kirk Arndt ; Vincent Riot ; Enver Alagoz ; Alec Biccum ; Andy Bohn ; Joseph Clampit ; Tony Coiro ; Wei Cui ; Liz Hoffman ; Alan Lichti ; Desiree Skaggs ; Ian Shipsey ; Matt Triano ; Bo Xin ; Kat Ziegler ; John Oliver ; Richard Van Berg ; Gunther Haller ; Leonid Sapozhnikov ; Scot Olivier; The LSST camera corner raft conceptual design: a front-end for guiding and wavefront sensing. Proc. SPIE 7736, Adaptive Optics Systems II, 773662 (July 28, 2010); doi:10.1117/12.857829.

[2] Anastacia M. Manuel, Donald W. Phillion, Scot S. Olivier, Kevin L. Baker, and Brice Cannon, "Curvature wavefront sensing performance evaluation for active correction of the Large Synoptic Survey Telescope (LSST)," Opt. Express 18, 1528-1552 (2010)

[3] D. W. Phillion, S. S. Olivier, K. Baker, L. Seppala, and S. Hvisc, "Tomographic wavefront correction for the LSST," Proc. SPIE 6272, 627213 (2006)

[4] Michael Warner ; Vincent Riot ; Jacques Sebag; LSST Telescope guider loop requirements analysis and predicted performance. Proc. SPIE 7738, Modeling, Systems Engineering, and Project Management for Astronomy IV, 77381U (August 03, 2010); doi:10.1117/12.858287

[5] Yibin Bai ; William Tennant ; Selmer Anglin ; Andre Wong ; Mark Farris ; Min Xu ; Eric Holland ; Donald Cooper ; Joseph Hosack ; Kenneth Ho ; Thomas Sprafke ; Robert Kopp ; Brian Starr ; Richard Blank ; James W. Beletic ; Gerard A. Luppino; 4K×4K format 10μm pixel pitch H4RG-10 hybrid CMOS silicon visible focal plane array for space astronomy. Proc. SPIE 8453, High Energy, Optical, and Infrared Detectors for Astronomy V, 84530M (September 25, 2012); doi:10.1117/12.926748

[6] Markus Loose ; James Beletic ; John Blackwell ; James Garnett ; Selmer Wong ; Don Hall ; Shane Jacobson ; Marcia Rieke ; Greg Winters; The SIDECAR ASIC: focal plane electronics on a single chip. Proc. SPIE 5904, Cryogenic Optical Systems and Instruments XI, 59040V (August 18, 2005); doi:10.1117/12.619638

[7] Lebbolo H., Tocut V., Antilogus P., Juramy C., Russo S.; CABAC : A CCD Clocking and Biasing Chip for LSST Camera. 2013 IEEE Nuclear Science Symposium and Medical Imaging Conference, and Room-Temperature Semiconductor X-Ray and Gamma-Ray Detectors workshop, Corée, République De (2013)

[8] P. Antilogus, Ph. Bailly, J. Jeglot, C. Juramy, H. Lebbolo, D. Martin, M. Moniez, V. Tocut and F. Wicek; LSST camera readout chip ASPIC: test tools. Topical Workshop on Electronics for Particle Physics 2011, 26–30 September 2011, Vienna, Austria

ACKNOWLEDGMENTS

LSST is a public-private partnership. Funding for design and development activity comes from the National Science Foundation, private donations, grants to universities, and in-kind support at Department of Energy laboratories and other LSSTC Institutional Members. This work is supported by in part the National Science Foundation under Scientific Program Order No. 9 (AST-0551161) and Scientific Program Order No. 1 (AST-0244680) through Cooperative Agreement AST-0132798. Portions of this work are supported by the U.S. Department of Energy under contract DE-AC02-76SF00515 with the Stanford Linear Accelerator Center, contract DE-AC02-98CH10886 with Brookhaven National Laboratory, with the Lawrence Livermore National Laboratory under the auspices of the U.S. Department of Energy under Contract DEAC52-07NA27344 and in part by the U.S. Department of Energy Office of High Energy Physics under grant DE-FG02-91ER40681A29 awarded to Purdue University. Portion of this work was also supported in part by Purdue University. Additional funding comes from private donations, grants to universities, and in-kind support at Department of Energy laboratories and other LSSTC Institutional Members.

This document was prepared as an account of work sponsored by an agency of the United States government. Neither the United States government nor Lawrence Livermore National Security, LLC, nor any of their employees makes any warranty, expressed or implied, or assumes any legal liability or responsibility for the accuracy, completeness, or usefulness of any information, apparatus, product, or process disclosed, or represents that its use would not infringe privately owned rights. Reference herein to any specific commercial product, process, or service by trade name, trademark, manufacturer, or otherwise does not necessarily constitute or imply its endorsement, recommendation, or favoring by the United States government or Lawrence Livermore National Security, LLC. The views and opinions of authors expressed herein do not necessarily state or reflect those of the United States government or Lawrence Livermore National Security, LLC, and shall not be used for advertising or product endorsement purposes.